1952 *Macromolecules* **2008,** *41,* 1952−1960

Multiblock Polysilane Copolymers: One-Pot Wurtz Synthesis, Fluoride Anion-Induced Block-Selective Scission Experiments, and Spectroscopic Characterization

Takuma Kawabe, Masanobu Naito, and Michiya Fujiki*

Graduate School of Materials Science, Nara Institute of Science and Technology, 8916-5 Takayama, Ikoma, Nara 630-0192, Japan

Received November 28, 2007; Revised Manuscript Received January 15, 2008

ABSTRACT: This paper reports the spontaneous formation of a high-molecular weight multiblock PSi copolymer made up of *i*-butyl-*n*-decyldichlorosilane (M**1**) and methyl-3,3,3-trifluoropropyldichlorosilane (M**2**). The copolymer was formed under conditions of simultaneous addition via a Wurtz-type condensation reaction with sodium in refluxing toluene, without the help of a cocatalyst. The multiblock structure of poly[(*i*-butyl-*n*-decylsilane)$_x$-*b*-(methyl-3,3,3-trifluoropropylsilane)$_{1-x}$] (PSi**1**) was characterized by means of ^{29}Si{^{1}H} NMR, UV absorption, photoluminescence (PL), and photoluminescence excitation (PLE) measurements. The average block lengths (L) of the *i*-butyl-*n*-decylsilane (Si**3**) block and the methyl-3,3,3-trifluoropropylsilane (Si**4**) block in PSi**1** were successfully evaluated by a block-selective scission technique using tetra-*n*-butylammonium fluoride (TBAF). This technique allowed for the selective decomposition of Si**4** in PSi**1** under reaction conditions when the concentration of TBAF and reaction time were optimal. The L values of Si**3** and Si**4** were, respectively, ∼4.8 nm (corresponding to an averaged repeating unit of $n \sim 26$) and ∼3.5 nm ($n \sim 19$). The copolymerization mechanism of PSi**1** was further studied using the time−conversion curves of M**1** and M**2** by gas chromatography. Gel permeation chromatography using a photodiode array UV detector and ^{1}H NMR measurements were used to analyze the PSi**1** product. Upon simultaneous addition of M**1** and M**2** comonomers, only M**2** initially formed the Si**4** oligomer ($M_n \sim 3\,000$), and after a certain period of polymerization time, M**1** abruptly copolymerized with the Si**4** oligomer, followed by formation of the multiblock PSi**1** copolymer.

Introduction

Soluble organopolysilanes (PSis) have received a great deal of attention for their potential applications as functional materials[1−3] in semiconductors,[4] radical photoinitiators,[5] precursors of silicon carbide,[6,7] and sensors.[8−10] In general, the Wurtz-type condensation reaction of diorganodichlorosilanes with sodium (the so-called, Wurtz synthesis) in refluxing toluene is known to be the most widely used method for the synthesis of alkyl/aryl-substituted PSis in appreciable yields.[1,2] This procedure is also applicable to constructing various PSi copolymers with the corresponding dichlorosilane comonomers (Scheme 1).[1] It was previously reported that multiblock PSi copolymers can be made by the modified Wurtz condensation reactions of comonomers, involving either sequential or simultaneous addition. In the former approach, PSi species with polymerizable reactive end(s) are initially produced by the addition of monomer A, followed by cocondensation upon the addition of monomer B.[11] As an alternative approach to obtain well-defined multiblock PSis, well-defined α,ω-dichlorosilane oligomers can be reacted with 1,5-dilithiodecaphenylpentasilane.[12] This approach, however, may be difficult to apply to the synthesis of a variety of multiblock PSis with high molecular weight. In contrast to sequential addition, simultaneous addition of two monomers can lead to the spontaneous formation of PSi copolymers with multiblock.[14−17] The investigators in these studies found that differences in the Na-mediated reduction reaction between two diorganodichlorosilane monomers is responsible for the formation of multiblock PSis. However, other details of the mechanism by which Wurtz cocondensation and polymerization lead to multiblock PSis and more detailed characterization of the multiblock lengths remain unclear.[11,13,16]

Scheme 1. Wurtz-Type Cocondensation Reaction of Dichlorodiorganosilane Comonomers for the Synthesis of Polysilane Copolymers

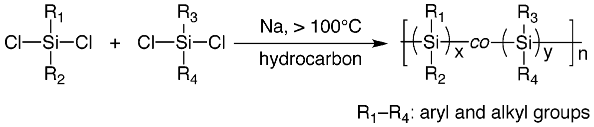

Until now, ^{29}Si and/or ^{13}C NMR experiments have suggested that the Wurtz approach with simultaneous addition of the following pairs of comonomers lead to blocklike copolymers: methylphenyldichlorosilane and *n*-hexylmethyldichlorosilane,[14] dimethyldichlorosilane and di-*n*-hexyldichlorosilane,[15,16] and methyl-*n*-propyldichlorosilane and methyl-3,3,3-trifluoropropyldichlorosilane.[17] The fact that NMR is the only available block-selective structural analysis technique has limited understanding of the copolymerization mechanism and of certain structural details (block lengths and block junctions) of blocklike PSis.

The present work takes advantage of the high reactivity and affinity between Si and fluoride anions (F$^-$) in order to evaluate the block lengths in a PSi copolymer produced by a Wurtz cocondensation reaction of fluoroalkyl-methyldichlorosilane and dialkyldichlorosilane.[18] This idea is based on previous reports that, in several disilanes, an Si−Si bond is cleaved by the attack of an F$^-$ in hexamethylphosphoric triamide to produce a metal-free silyl anion and triorganosilylfluoride.[19,20] Hiyama et al. showed that the F$^-$ selectively attacks the less sterically hindered Si atom of these disilanes, followed by an electronically favored silyl anion. On the other hand, in a polymer system, we have reported that an F$^-$ of tetra-*n*-butylammonium fluoride (TBAF) can weakly coordinate with the Si main chain of poly(methyl-

---

* To whom correspondence should be addressed. E-mail: fujikim@ms.naist.jp.

10.1021/ma702639f CCC: $40.75

Scheme 2. Chemical Structures of Polysilane Copolymers and Homopolymers Used in This Study; PSi1, Poly[(*i*-butyl-*n*-decylsilane)$_x$-*co*-(methyl-3,3,3-trifluoropropylsilane)$_{1-x}$]; PSi2, Poly[(*i*-butyl-*n*-decylsilane)$_x$-*co*-(methyl-*n*-propylsilane)$_{1-x}$]; PSi3, Poly(*i*-butyl-*n*-decylsilane); PSi4, Poly(methyl-3,3,3-trifluoropropylsilane); PSi5, Poly(methyl-*n*-propylsilane)

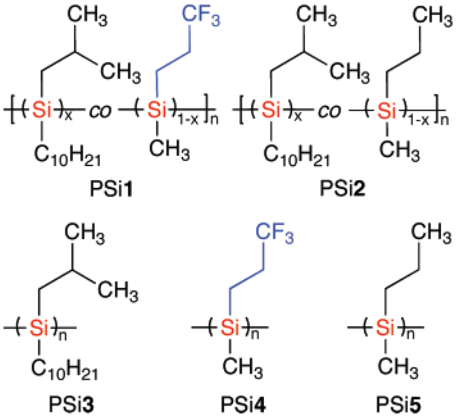

3,3,3-trifluoropropylsilane) (PSi**4**, Scheme 2), inducing a cooperative change in the semiflexible-to-coil conformation of PSi**4**.[8,9] We reasoned that, by utilizing these specific interactions and reactions between Si and F$^-$, an F$^-$ with an Si main chain in either block of the blocklike PSi copolymer might cause block-selective scission under carefully controlled concentration and reaction time conditions at ambient temperature. If either block were selectively scissible, it would be possible to directly evaluate the block length of the other block by conventional polymer characterization techniques, such as gel permeation chromatography (GPC), NMR, and UV spectroscopy.

Using the above approach and idea, we were able to successfully characterize the average block lengths of *i*-butyl-*n*-decylsilane (Si**3**) and methyl-3,3,3-trifluoropropylsilane (Si**4**) blocks incorporated in poly[(*i*-butyl-*n*-decylsilane)-*co*-(methyl-3,3,3-trifluoropropylsilane)] (PSi**1**, Scheme 2). To do this, we followed several steps. First, the blocklike nature of the PSi**1** main chain was confirmed by means of ^{29}Si{^{1}H} NMR, UV absorption, photoluminescence (PL), and photoluminescence excitation (PLE) measurements. Second, poly(*i*-butyl-*n*-decylsilane) (PSi**3**, Scheme 2) and PSi**4** homopolymers were used to optimize the selective scission reaction conditions of PSi**1**. Third, the block lengths of the Si**3** and the Si**4** block in PSi**1** were evaluated using ^{29}Si{^{1}H} NMR, ^{1}H NMR, FT-IR measurements, and GPC equipped with a photodiode array UV detector. Finally, two types of time−conversion curves were obtained for the dichlorosilane comonomers by gas chromatography (GC) and for the polymer products by GPC and ^{1}H NMR. On the basis of these experimental results and analyses, we propose that the block copolymerization mechanism of PSi**1** is a Wurtz synthesis, i.e., a Wurtz-type cocondensation reaction with sodium.

Experimental Section

Measurements. The number-averaged molecular weight of the polymer (M_n) was evaluated at 40 °C using a Shimadzu A10 GPC apparatus equipped with a column containing PLgel 10 μm mixed-B (Polymer Laboratories) and a photodiode array UV detector. Tetrahydrofuran (THF) was used as the eluent. The column was calibrated with polystyrene standards. GC was performed on a Shimadzu GC-2010 chromatograph using a DB-1HT column (Agilent). UV absorption spectra were recorded on a JASCO V-550 spectrophotometer. PL and PLE spectra were measured using a JASCO FP-6500 spectrofluorometer. ^{1}H and ^{13}C{^{1}H} NMR spectra were measured in CDCl$_3$ with a JEOL JNM-LA400 spectrometer using tetramethylsilane (Me$_4$Si) (δ 0.0 ppm) as an internal standard. ^{29}Si{^{1}H} NMR spectra were measured with a JEOL JNM-LA400 spectrometer in CDCl$_3$ and THF-d_8, using Me$_4$Si and hexamethyldisilane (HMDS) (δ −19.7 ppm) as the internal standards, respectively. ^{19}F NMR spectra were measured with a JEOL JNM-ECP600NK spectrometer in THF-d_8 using benzotrifluoride (δ −64.0 ppm) as an internal standard. FT-IR spectra were obtained on a Horiba FT-730 by casting a THF and CDCl$_3$ solution of PSis onto a KBr substrate.

Table 1. Sample Data for Poly(*i*-butyl-*n*-decylsilane) (PSi3)

fraction	M_n[a] ($\times 10^{-5}$)	PDI[b]	yield (%)
1	11	2.2	2.7
2	2.8	5.2	2.0
3	2.1	3.9	0.2
4	1.4	4.8	1.1
5	1.6	1.6	1.2
6	0.85	1.3	1.2
7	0.57	1.2	1.7
8	0.38	1.2	1.2
9	0.30	1.2	0.8
10	0.25	1.2	0.6

[a] M_n = number-average molecular weight. [b] PDI = polydispersity index (M_w/M_n).

Monomer Preparation. The dialkylsilane monomer, *i*-butyl-*n*-decyldichlorosilane (M**1**), was synthesized as follows. First, 1-bromodecane (TCI, 25.2 g, 114 mmol) was reacted with magnesium (Wako, 3.28 g, 135 mmol) in dry THF (Wako, 80.0 mL) for 1 h at 80 °C. The Grignard reagent was added to *i*-butyltrichlorosilane (Shin-Etsu, 20.0 g, 104 mmol) in a mixture of dry THF (80.0 mL) and diethylether (Wako, 300 mL) at 35 °C. After 12 h, the salts were removed by filtration from the reaction mixture. The crude product was purified by vacuum distillation to yield the desired monomer as a colorless liquid, with 54.0% yield (17.0 g). The boiling point was determined to be 117−120 °C (8.0 Torr). ^{1}H NMR results (399.00 MHz, CDCl$_3$) were as follows (ppm): 0.88 (t, −CH$_2$−*CH$_3$*), 1.02 (d, −CH−*CH$_3$*), 1.09 (m, −Si−*CH$_2$*−), 1.26 (m, −*CH$_2$*−), 1.50 (m, −Si−CH$_2$−*CH$_2$*−CH$_2$−), 2.00 (m, −*CH*−CH$_3$). ^{13}C NMR results (100.00 MHz, CDCl$_3$) were as follows (ppm): 14.1, 21.3, 22.4, 22.7, 24.2, 25.6, 29.1, 29.3, 29.4, 29.6, 30.4, 31.9, 32.5. ^{29}Si NMR (79.00 MHz, CDCl$_3$) showed a single peak at 32.6 ppm.

Methyl-3,3,3-trifluoropropyldichlorosilane (M**2**) and methyl-*n*-propyldichlorosilane (M**3**) were purchased from Shin-Etsu and purified by vacuum distillation prior to polymerization.

Polymer Preparation. All reactions were carried out in dried glassware under a dry nitrogen gas atmosphere. Details of the homopolymer synthesis (PSi**3**, PSi**4**, and PSi**5**) have already been described in previous papers.[21−24] It is known that addition of a catalytic amount of 18-crown-6 and 15-crown-5 to most reactions of dialkyldichlorosilanes with sodium in hot toluene reproducibly leads to high yields of high-molecular weight PSis showing a monomodal distribution.[25,26] However, we have shown that several alkyl-3,3,3-trifluoropropyldichlorosilanes are exceptions to this rule; they do not produce the corresponding PSi homopolymers when crown ethers are present in the reaction mixture.[9,23,24] Similarly, in the present study, using 18-crown-6 in the Wurtz cocondensation of M**1** and M**2** did not lead to the production of PSi**1** or PSi**4**. The sample data for PSi**3**, PSi**4**, and PSi**5** are shown in Tables 1−3.

Poly[(*i*-butyl-*n*-decylsilane)$_x$-*co*-(methyl-3,3,3-trifluoropropylsilane)$_{1-x}$] (PSi**1**) was prepared as follows. A freshly distilled mixture of M**1** (2.70 g, 9.10 mmol) and M**2** (1.90 g, 9.10 mmol) was added dropwise to 0.84 g (36.0 mmol) of sodium (Wako) suspended in 10.0 mL of refluxing toluene (Wako) and vigorously stirred under atmospheric nitrogen at 120 °C. After 2 h, 90.0 mL of dry toluene (Wako) was added to reduce the solution viscosity, and stirring was continued for an additional 1 h at 100 °C. The hot reaction mixture was immediately passed through a PTFE filter (2 μm pore size; Sumitomo Electric) under nitrogen

Table 2. Sample Data for Poly(methyl-3,3,3-trifluoropropylsilane) (PSi4)

fraction	$M_n{}^a$ ($\times 10^{-4}$)	PDI^b	yield (%)
1	1.7	1.6	1.6
2	1.3	1.2	0.7
3	0.76	1.3	13

[a] M_n = number-average molecular weight. [b] PDI = polydispersity index (M_w/M_n).

Table 3. Sample Data for Poly(methyl-*n*-propylsilane) (PSi5)

fraction	$M_n{}^a$ ($\times 10^{-4}$)	PDI^b	yield (%)
1	3.1	1.6	2.7
2	1.8	1.7	2.4
3	1.5	1.6	2.0
4	1.3	1.5	4.6

[a] M_n = number-average molecular weight. [b] PDI = polydispersity index (M_w/M_n).

gas pressure. The precipitating solvents, 2-propanol, ethanol, and methanol, were carefully added to the clear filtrate. Several portions of white precipitate were collected by centrifugation and dried under vacuum at 80 °C. ^{1}H NMR (399.00 MHz, CDCl$_3$, ppm): 0.37 (br, $-\mathrm{Si}-\mathit{CH_3}$), 0.87 (t, $-\mathrm{CH_2}-\mathit{CH_3}$), 0.98 (br, $-\mathrm{Si}-\mathit{CH_2}-$, $-\mathrm{CH}-\mathit{CH_3}$), 1.10 (br, $-\mathrm{Si}-\mathit{CH_2}-\mathrm{CH_2}-\mathrm{CF_3}$), 1.26 (br, $-\mathit{CH_2}-$), 1.73 (br, $-\mathit{CH}-\mathrm{CH_3}$), 2.06 (br, $-\mathrm{Si}-\mathrm{CH_2}-\mathit{CH_2}-\mathrm{CF_3}$). ^{29}Si NMR (79.00 MHz, CDCl$_3$, ppm): -23.1 ($\mathit{Si}-\mathrm{CH_2}-\mathrm{CH(CH_3)}-\mathrm{CH_3}$), -31.7 ($\mathit{Si}-\mathrm{CH_2}-\mathrm{CH_2}-\mathrm{CF_3}$). ^{19}F NMR (564.69 MHz, CDCl$_3$, ppm): -69.9; FT-IR (cm^{-1}) 2955 (ν_{as}(CH$_3$)), 2925 (ν_{as}(CH$_2$)), 2872 (ν_s(CH$_3$)), 2855 (ν_s(CH$_2$)), 1262 (δ_s(SiCH$_3$)), 1214 (ν_{as}(CF)), 1198 (ν(CC)), 1130 (ν_s(CF)). For PSi**1**, the composition fractions were determined by ^{1}H NMR and the data is shown in Table 4.

Poly[(*i*-butyl-*n*-decylsilane)$_x$-*co*-(methyl-*n*-propylsilane)$_{1-x}$] (PSi**2**) was prepared as follows. A mixture of 0.92 g (40.4 mmol) of sodium metal and 0.05 g (0.20 mmol) of 18-crown-6 (Wako) in 10.0 mL of dry toluene was added dropwise to a mixture of M**1** (3.02 g, 10.1 mmol) and M**3** (1.58 g, 10.1 mmol) in a nitrogen gas atmosphere at 120 °C. After 1 h, 100 mL of dry toluene was added to reduce the solution viscosity, and stirring was continued for an additional 1 h at 100 °C. The hot reaction mixture was passed through a 2 μm PTFE filter under nitrogen gas pressure. The precipitating solvents, 2-propanol, ethanol, and methanol, were carefully added to the clear filtrate. Several portions of white precipitate were collected by centrifugation and dried under vacuum at 80 °C. ^{1}H NMR (399.00 MHz, CDCl$_3$, ppm): 0.25 (br, $-\mathrm{Si}-\mathit{CH_3}$), 0.85 (br, $-\mathrm{Si}-\mathit{CH_2}-\mathrm{CH_2}-\mathrm{CH_3}$), 0.87 (t, $-\mathrm{CH_2}-\mathit{CH_3}$), 0.98 (br, $-\mathrm{Si}-\mathrm{CH_2}-\mathrm{CH_2}-\mathit{CH_3}$, $-\mathrm{Si}-\mathit{CH_2}-$, $-\mathrm{CH}-\mathit{CH_3}$), 1.26 (br, $-\mathit{CH_2}-$), 1.37 (br, $-\mathrm{Si}-\mathrm{CH_2}-\mathit{CH_2}-\mathrm{CH_3}$), 1.78 (br, $-\mathit{CH}-\mathrm{CH_3}$). ^{29}Si NMR (79.00 MHz, CDCl$_3$, ppm): -23.0 ($\mathit{Si}-\mathrm{CH_2}-\mathrm{CH(CH_3)}-\mathrm{CH_3}$), -32.5 ($\mathit{Si}-\mathrm{CH_2}-\mathrm{CH_2}-\mathrm{CH_3}$). The data is shown in Table 5.

Evaluation of Average Block Length of PSi1. The molecular weight of PSis changed markedly upon addition of tetra-*n*-butylammonium fluoride (TBAF) to the reaction, as detected by GPC equipped with a photodiode array UV detector. To optimize the concentration of fluoride anion (F$^-$) in this block-selective scission, different concentrations of TBAF (1.0 M in THF solution, TCI) were added to the THF solution of PSi**3** or PSi**4** at room temperature (PSi**3**, 1.5 × 10^{-5} M; PSi**4**, 3.0 × 10^{-5} M). The concentration ratios tested were [F$^-$]/[Si repeat unit] = 0.5, 0.1, 0.05, 0.01, 0.005, and 0.001. GPC was used to evaluate the molecular weights of PSi**3** and PSi**4** 15 min after the addition of TBAF. Through these experiments, we were able to optimize the conditions for selective scission of PSi**4**. Under these reaction conditions, however, the molecular weight of PSi**3** remained unchanged.

Subsequently, we demonstrated selective scission of Si**4** blocks in PSi**1** based on the above optimized reaction conditions for PSi**3** and PSi**4** (Figure 1). Initially, the PSi**1** was dissolved in THF (1.8 × 10^{-3} M, 62 mL). TBAF was then added at room temperature to the THF solution of PSi**1** at a molar ratio of [F$^-$]/[Si repeat unit] = 0.5. After 15 min, the scission reaction was quenched by evaporating the THF solution. To obtain nondecomposed Si**3** blocks, the crude products obtained were extracted with methanol. This could be done because only the decomposed blocks of PSi**1** were dissolved in methanol. The insoluble portion was then dissolved in *n*-hexane (Wako). Structural characterization of these portions was carried out by GPC, NMR (^{1}H, ^{29}Si{^{1}H}, ^{19}F), and FT-IR measurements. It is important to note that ^{1}H NMR showed that the methanol-extracted portion contained TBAF only. On the other hand, plural NMR measurements (^{1}H, ^{29}Si{^{1}H}, ^{19}F) indicated the presence of unreacted Si**3** blocks and the absence of reacted Si**4** fractions in the *n*-hexane-portion.

Results and Discussion

Structural Characterization of PSi1. Figure 2 compares the ^{29}Si{^{1}H} NMR spectra of PSi**1**, PSi**3**, and PSi**4** (THF-d_8, internal reference: hexamethyldisilane). Chemical shifts of PSi**3** and PSi**4** appeared at -23.0 and -31.8 ppm, respectively, originating from the respective Si$-$Si backbones. In the case of PSi**1**, two NMR signals were clearly observed at -22.9 and -31.3 ppm, without any other signals. These peaks were almost identical to those of PSi**3** and PSi**4**, respectively. These results indicate that the main chain of PSi**1** is composed of blocklike structures, with long blocks of similar silicon repeating units, rather than random or alternating structures. The junctions between the Si**3** and Si**4** blocks probably belong to a small, undetectable fraction, compared to Si**3** and Si**4** blocks (see Figure S1 of the Supporting Information). In order to investigate the effect of a trifluoropropyl side chain in a Wurtz-type cocondensation reaction with sodium (Wurtz synthesis), PSi**2** was prepared for comparison. PSi**2** is regarded as a nonfluoroalkyl copolymer analogue of PSi**1**: it shows two NMR signals at similar chemical shifts to the corresponding homopolymers (see Figure S2). These results strongly suggest that the blocklike main chain structure of PSi**1** is unaffected by the fluoroalkyl side chain. In order to examine the generality of the blocklike nature in several dialkyldichlorosilane copolymers using ^{29}Si{^{1}H} NMR, we prepared three PSi copolymers: poly[(di-*n*-butylsilane)$_x$-*co*-(methyl-*n*-propylsilane)$_{1-x}$], poly[(diethylsilane)$_x$-*co*-(methyl-*n*-propylsilane)$_{1-x}$], and poly[(diethylsilane)$_x$-*co*-(di-*n*-butylsilane)$_{1-x}$] (see Figure S3). The ^{29}Si{^{1}H} NMR spectra of these three copolymers showed two broad peaks, as was the case with PSi**1** and PSi**2,** when compared to those of the corresponding homopolymers. These results indicate that formation of the blocklike structure in copolymers may be a common feature in Wurtz synthesis of dialkyldichlorosilane comonomers and may be caused by difference in how easily the different comonomers undergo Na-mediated reduction.

The blocklike nature of PSi**1** was further supported by UV, PL, and PLE measurements. It has previously been demonstrated that for various PSi derivatives, the longest wavelength (λ_{max}) and the full width at half-maximum (fwhm) of the UV absorption band due to the excitonic Si$\sigma-$Siσ^* transition provide information about both the local and global conformation in solution.[2] For example, the λ_{max} of poly(dialkylsilane)s with 2_1, 15_7, and 7_3 helices appears at ~370, 345, and 320 nm, respectively.[27] Figure 3 shows the UV absorption spectra of PSi**1**, PSi**3**, and PSi**4** in THF at 25 °C. PSi**3** has an intense, narrow UV absorption band at 320 nm with an fwhm of 692 cm^{-1}, which suggests that PSi**3** forms a semiflexible 7_3 helix (seven silicon atoms in three turns).[2,22] PSi**4** shows a broad, weak UV absorption peak around 280 nm with an fwhm of 4794 cm^{-1} originating from random coil and/or globulelike structures.[24] On the other hand, PSi**1** shows UV absorption at 313 nm with an fwhm of 2655 cm^{-1}, with an intermediate intensity and fwhm between that of PSi**3** and PSi**4**. These results suggest that PSi**1** consists of a semiflexible 7_3-helical domain

Table 4. Sample Data for Poly[(*i*-butyl-*n*-decylsilane)$_x$-*co*-(methyl-3,3,3-trifluoropropylsilane)$_{1-x}$] (PSi1)

fraction	feed mol fraction [MA (mol)/MF (mol)]	product mol fraction[c] [MA (mol)/MF (mol)]	M_n[a] ($\times 10^{-5}$)	PDI[b]	yield (%)
1	0.50/0.50	0.56/0.44	4.3	3.5	2.7
2	0.50/0.50		4.8	2.7	3.2
3	0.50/0.50	0.57/0.43	2.9	2.5	4.1
4	0.50/0.50		1.8	2.0	1.1
5	0.50/0.50	0.55/0.45	1.0	1.9	0.9

[a] M_n = number-average molecular weight. [b] PDI = polydispersity index (M_w/M_n). [c] The composition fractions were determined by ^{1}H NMR measurements.

Table 5. Sample Data for Poly[(*i*-butyl-*n*-decylsilane)$_x$-*co*-(methyl-*n*-propylsilane)$_{1-x}$] (PSi2)

fraction	feed mol fraction [MA$_1$ (mol)/MA$_2$ (mol)]	product mol fraction[c] (x (mol)/1 − x (mol))	M_n[a] ($\times 10^{-5}$)	PDI[b]	yield (%)
1	0.50/0.50		10	3.6	0.6
2	0.50/0.50		10	2.3	3.2
3	0.50/0.50	0.27/0.73	3.1	2.3	1.9
4	0.50/0.50		2.4	1.8	1.5
5	0.50/0.50		2.0	1.8	1.4
6	0.50/0.50		1.6	1.5	1.1
7	0.50/0.50	0.42/0.58	1.2	1.7	3.3
8	0.50/0.50		0.98	1.4	1.2
9	0.50/0.50		0.75	1.7	1.4
10	0.50/0.50		0.48	1.8	2.3
11	0.50/0.50		0.39	1.5	2.9
12	0.50/0.50		0.34	1.5	1.8
13	0.50/0.50		0.30	1.4	1.9
14	0.50/0.50		0.21	1.5	0.9

[a] M_n = number-average molecular weight. [b] PDI = polydispersity index (M_w/M_n). [c] The composition fractions were determined by ^{1}H NMR measurements.

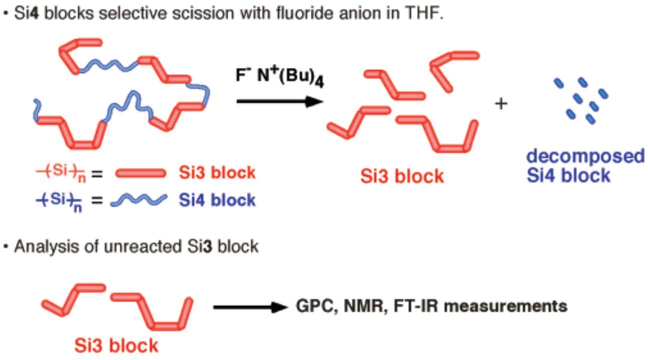

Figure 1. Schematic illustration of the block-selective scission experiment for Si**4** blocks incorporated in PSi**1**.

and a random coil or globulelike domain. This was further supported by the following PL and PLE experiments and by the analysis of PSi**1**.

Figure 4 compares the PL and PLE spectra of PSi**1**, PSi**3**, and PSi**4** in THF solution at 25 °C. The narrow PL and PLE bands of PSi**3** have intense signals at 323 nm (excited at 315 nm) with an fwhm of 972 cm^{-1} and at 318 nm (monitored at 324 nm) with an fwhm of 885 cm^{-1}. A very small Stokes shift of 484 cm^{-1} indicates the existence of a fairly uniform fluorescent center in PSi**3**. These spectroscopic features are characteristic of semiflexible PSis. On the other hand, the random coil/globulelike nature of PSi**4** is indicated by a broad PL band peaking at 333 nm (excited at 291 nm) with an fwhm of 2137 cm^{-1} and a PLE band at 304 nm (monitored at 333 nm) with an fwhm of 3398 cm^{-1}. A very large Stokes shift of 2817 cm^{-1} indicates the existence of disordered fluorescent centers in PSi**4**.

Note that the apparent PL band of PSi**1** appears at 333 nm (excited at 280 nm) with an fwhm of 2410 cm^{-1}, very similar to that of PSi**4**. However, the PLE spectrum (monitored at 315 nm) contains three major peaks located at 288, 304, and 312 nm. The two PLE peaks at 304 and 312 nm are almost identical to those of PSi**4** and PSi**3**, respectively, while the origin of the PLE peak at 288 nm is unclear. On the other hand, the PLE spectral shapes monitored at 335 and 375 nm are quite different from that monitored at 315 nm (see Figure S4). This suggests that photoexcited energy migration does not occur effectively in the main chain comprising multiblocks (see Figure S4). The 288 nm band is inferred to originate from the junction-related or highly disordered structures between Si**4** and Si**3** blocks. Measurements by all of these techniques, ^{29}Si{^{1}H} NMR, UV, PL, and PLE, are consistent with the hypothesis that the main chain of PSi**1** adopts multiblock structures.

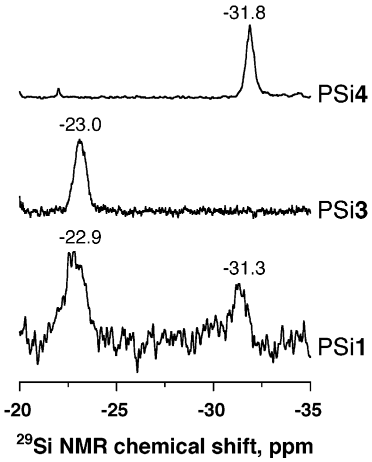

Figure 2. ^{29}Si{^{1}H} spectra of PSi**1** (M_n = 6.9 × 10^5, PDI = 2.3), PSi**3** (M_n = 4.1 × 10^4, PDI = 1.6), and PSi**4** (M_n = 7.6 × 10^3, PDI = 1.3) in THF-d_8 at room temperature. Hexamethyldisilane (HMDS) was used as an internal reference.

Si−Si Main Chain Decomposition of PSi3 and PSi4 with TBAF. The first step in the block-selective scission experiments of Si**3** or Si**4** blocks incorporated in multiblock PSi**1** with TBAF was to find the optimal decomposition conditions for PSi**3** and PSi**4** with TBAF. Decomposition was determined by GPC

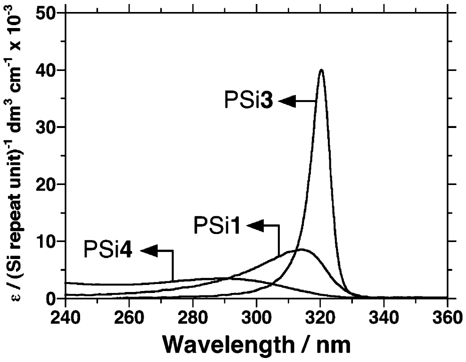

Figure 3. UV absorption spectra of PSi**1** ($M_n = 1.6 \times 10^5$, PDI = 2.2, $\sim 10^{-5}$ M), PSi**3** ($M_n = 1.4 \times 10^5$, PDI = 1.8, $\sim 10^{-5}$ M), and PSi**4** ($M_n = 1.6 \times 10^4$, PDI = 1.6, $\sim 10^{-4}$ M) in THF at 25 °C.

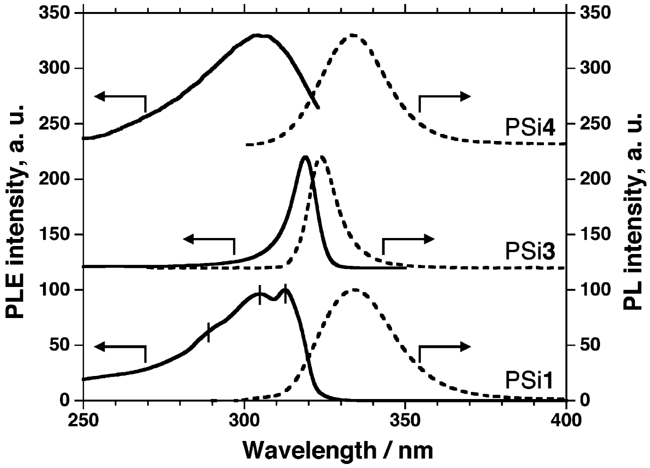

Figure 4. PL and PLE spectra of PSi**1** ($M_n = 1.6 \times 10^5$, PDI = 2.2, excited at 280 nm, monitored at 315 nm), PSi**3** ($M_n = 2.2 \times 10^4$, PDI = 3.5, excited at 315 nm, monitored at 324 nm), and PSi**4** ($M_n = 7.6 \times 10^3$, PDI = 1.3, excited at 291 nm, monitored at 333 nm) in THF ($\sim 10^{-5}$ M) at 25 °C.

measurements. First, PSi**3** and PSi**4** were dissolved in THF at concentrations of 1.5×10^{-5} M and 3.0×10^{-5} M, respectively. TBAF was then added to the solutions for 15 min at room temperature and the ratio between fluoride anion (F^-) and PSi ($[F^-]$/[Si repeat unit]) was varied (see Figure S5). The M_n value of PSi**4** immediately decreased upon the addition of TBAF, and PSi**4** decomposed completely at concentrations above 5 mol %. On the other hand, the M_n value of PSi**3** did not change even though the reaction was identical to that carried out on PSi**4**. Thus, when the ratio of $[F^-]$/[Si repeat unit] was greater than 5 mol %, it was possible to selectively decompose only the Si**4** block with TBAF. This knowledge was applied to evaluate the block lengths of Si**3** and Si**4** for PSi**1**.

Si4 Block-Selective Scission of PSi1 with TBAF. Figure 5a shows the change in the M_n value with the addition of TBAF (50 mol %) to PSi**1** in THF (1.8×10^{-3} M). The value of M_n drastically decreased from 1.6×10^5 to 6.0×10^3 for 15 min after the addition of TBAF. However, the λ_{max} value of PSi**1** was slightly red-shifted from 310 to 315 nm (see Figure S6). Because the λ_{max} value of PSi**3** is 320 nm, this red-shift implies that the Si**4** block in PSi**1** was selectively decomposed by TBAF. This was proven by the ^{29}Si and ^{1}H NMR spectra of TBAF-unreacted PSi residues. Figure 5b compares the ^{29}Si{^{1}H} NMR spectra obtained in $CDCl_3$ at room temperature of PSi**3** ($M_n = 3.8 \times 10^4$, PDI = 1.2) and unreacted residues extracted from THF solution. Although PSi**3** had a single resonance at -23.2 ppm with a broad line width ($\nu_{1/2} \sim 64$ Hz), which is characteristic of semiflexible PSis with limited main chain mobility,[21] unreacted residues showed a single resonance at -21.9 ppm with a narrow line width ($\nu_{1/2} \sim 4.8$ Hz), suggesting isolation of Si**3** blocks with a sufficiently high mobility in the main chain. These results lead to the conclusion that the Si**4** block in PSi**1** can be selectively decomposed by F^- under controlled conditions.

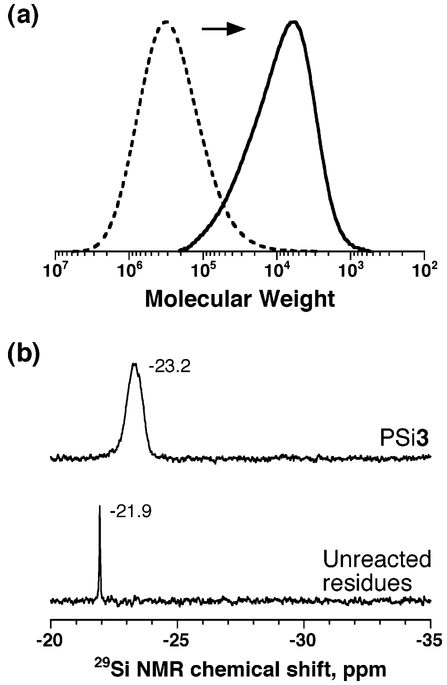

Figure 5. (a) Changes in the molecular weight upon the addition of TBAF to PSi**1** ($M_n = 1.6 \times 10^5$, PDI = 2.5, 1.8×10^{-3} M) in THF at room temperature; without addition (dashed line) and 15 min after the addition of TBAF ($[F^-]$/[Si repeat unit] = 0.5, solid line). (b) ^{29}Si{^{1}H} NMR spectra of PSi**3** ($M_n = 3.8 \times 10^4$, PDI = 1.2) and unreacted residues in $CDCl_3$ at room temperature. Tetramethylsilane (TMS) was used as an internal reference.

Additional ^{1}H NMR experiments support this conclusion. Figure S7 compares ^{1}H NMR spectra of PSi**1**, PSi**3**, PSi**4**, and the unreacted residues. The unreacted PSi species were assigned to the Si**3** block structure itself. A new signal at ~0.5 ppm in the ^{1}H NMR spectra of the unreacted residues was assigned to the methylene group in $SiCH_2-$ of Si**3** on the basis of further ^{1}H−^{1}H COSY measurements (data not shown). The other ^{1}H signals at ~0.1 and ~2.1 ppm are likely due to the Si**4** moiety. This is because these signals are similar to those of PSi**4,** as suggested by a comparison between ^{1}H and ^{19}F NMR spectra [see Figures S7 and S8a]. On the basis of the integration of ^{1}H NMR signals, the fraction of the Si**4** moiety in the Si**3** block is estimated to be as small as ~11 mol %. These results suggest that Si**4** moieties exist at the ends of the Si**3** blocks and/or between them. FT-IR also revealed three intense signals at 1087, 1028, and 800 cm^{-1} attributable, respectively, to $\nu_{as}(Si-O-CH_3)$, $\delta(Si-OH)$, and $\nu_s(Si-O-CH_3)$ of Si**3** blocks [see Figure S8b]. In contrast, careful analysis by ^{19}F NMR failed to detect any signals due to Si−F bonds located at the chain end(s) of the Si**3** blocks. Nevertheless, these NMR and IR results imply that the chain end(s) of the Si**3** blocks are Si−F bonds following successful Si**4** block-selective scission by F^-. It is possible that the Si−F bonds on the chain end(s) may easily turn into $Si-OCH_3$ and/or Si−OH bonds by extracting the unreacted residues from the reaction mixture with methanol.

Average Lengths of Si3 and Si4 Blocks in PSi1. After establishing block-selective scission of PSi**1** with TBAF, we analyzed M_n, average number of Si repeat units (n), and average length (L) of the Si**3** and Si**4** blocks in multiblock PSi**1**. First, the values of M_n and n for the Si**3** blocks were evaluated using GPC analysis and found to be 6 000 and 26, respectively. The L value of Si**3** (∼4.8 nm) was calculated as the product of n for the Si**3** block and the contour length of the 7_3 helical structure of Si**3** (0.185 nm).[22] To evaluate L for the decomposed Si**4** blocks, we assumed that the Si**3** and Si**4** blocks alternately coexist in the main chain of PSi**1**. The calculated values of M_n and n for the Si**4** block were 2 600 and 19, respectively, which were determined by taking into account the composition fractions of PSi**1** ($x = 0.57$, determined by ^{1}H NMR analysis). The value of L for the Si**4** block was therefore ∼3.5 nm. This analysis suggests that PSi**1** consists of Si**3** and Si**4** blocks of relatively short length.

We propose two explanations for the F^- induced Si**4** block-selective scission reaction. One is based on the difference in steric effect around Si atoms in Si**3** vs Si**4** blocks. Si**4** blocks have small, compact methyl groups, whereas Si**3** blocks have flexible long *n*-decyl side groups that may protect from nucleophilic attack by F^-. The compact methyl groups in Si**4** blocks are likely to make its Si−Si bonds highly reactive to nucleophilic attack. The second explanation is based on electronic differences between Si**3** and Si**4** blocks. The electron-withdrawing trifluoropropyl side chains are likely to play a key role in Si**4** block-selective scission experiments. The ^{1}H NMR signal of the methylene group in Si**4** blocks in PSi**1** (Si*CH*$_2$-CH$_2$CF$_3$, 1.10 ppm) was slightly downfield-shifted compared to the signal of the methylene group in Si**3** blocks (Si*CH*$_2$−, 0.98 ppm). This result suggests that the electron density of the Si main chain is affected through three single bonds by three electron-withdrawing F atoms located at remote positions. Recently, using computational calculation, Zhang et al. showed the mechanism of hydrogen passivation on Si surfaces by HF molecules.[28] For silicon surfaces terminated with three fluorine atoms, the polarization induced by the F-bonded moieties causes the neighboring Si−Si bonds to exhibit a high degree of ionic character, thereby facilitating attack by highly polar HF molecules. Therefore, the Si**3** and Si**4** blocks may show a large difference in reactivity to attack by F^-. This possibility is strongly supported by computational calculations in which the Gaussian 03/AM1 algorithm (Gaussian) is applied to models of PSi**1** and PSi**2** diblock structures: (*i*-butyldiethylsilane)$_5$-(methyl-3,3,3-trifluoropropylsilane)$_5$ (model **1**) and (*i*-butyldiethylsilane)$_5$- (methyl-*n*-propylsilane)$_5$ (model **2**). Prior to these calculations, the geometries of the diblock models were optimized by molecular mechanics (Materials Studio 4.0 with PCFF as a force field, Accelrys, San Diego CA). The HOMO charge density localizes to the *i*-butyldiethylsilane pentamer site, while conversely, the LUMO charge density localizes to a methyl-3,3,3-trifluoropropylsilane pentamer site (see Figure S9). For these calculations, the LUMO level of Si**4** blocks in PSi**1** was assumed to be significantly stabilized and Si**4** blocks to have more positive charges than the Si**3** blocks. In the case of model **2**, the HOMO charge density is delocalized over both the *i*-butyldiethylsilane and methyl-*n*-propylsilane sites and the LUMO charge density is delocalized over the *i*-butyldiethylsilane pentamer site, as well as the methyl-*n*-propylsilane pentamer site (see Figure S10). These calculations support the second explanation that the electron-withdrawing trifluoropropyl groups strongly affect the degree of localization at the LUMO level, which may be responsible for the Si**4** block-selective scission induced by F^-.

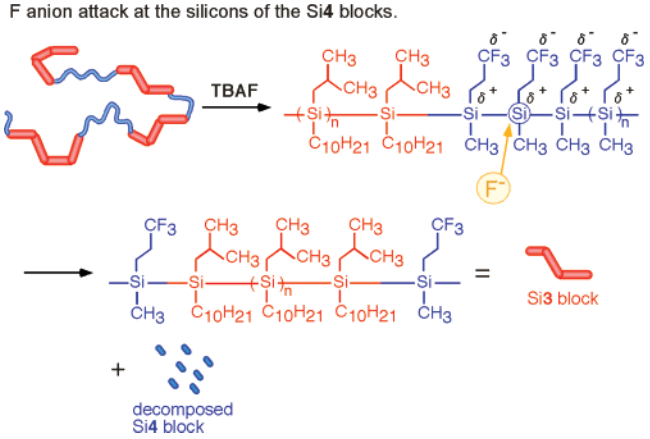

Figure 6. Schematic illustration of selective scission of an Si**4** block with a fluoride anion in THF at room temperature.

Thus, Si**4** blocks in Si**3**/Si**4**-block PSi**1** can be selectively attacked by an F^-, leading to Si**4** block-selective decomposition/scission reactions in the main chain. The nature of the positively charged Si atoms in the Si**4** block may facilitate effective attack by F^- to produce even shorter Si**4** residues at the end of Si**3** blocks (Figure 6).

Multiblock Copolymerization Mechanism of PSi1. In order to elucidate the mechanism of multiblock PSi**1** copolymerization in a one-pot Wurtz synthesis, we obtained time−conversion curves of M**1** and M**2** by GC analysis, as well as time−conversion curves of polymer products. The products were further characterized by GPC and ^{1}H NMR. Figure 7A shows the time−conversion curves of M**1** and M**2** for reaction times 1−2 h in toluene at 120 °C. Conversions were calculated based on crude total yields prior to the separation of oligomers into low-molecular weight (LMW) and high-molecular weight (HMW) fractions. It is evident that ∼50% of M**2** was selectively and rapidly consumed during the first 20 min and completely consumed after 60 min. However, M**1** hardly reacted with sodium for the first 20 min period but was gradually consumed between 20 and 60 min, reaching ∼50% consumption after 60 min. M**2** and M**1** thus showed very different chemical reactivity to sodium.

Figure 7B,C shows changes in the M_n values of the products with polymerization time. These plots were obtained from the relative intensity of UV bands around 244 nm (oligomer), 292−295 nm (Si**4** oligomer), 300 nm (PSi**1**), and 303−311 nm (PSi**1**), based on three-dimensional GPC chromatograms including UV absorption spectra collected at each elution time. The UV absorption bands of products (b and c) were red-shifted with increasing M_n. The products responsible for the 292−295 nm UV band existing in the initial 20 min polymerization period could be assigned to the Si**4** oligomer ($M_n = 3\,000$, $n = 21$) based on ^{1}H NMR measurements. The 244 nm UV band may be due to cyclic oligosilanes formed by end-biting and back-biting reactions. In contrast, the Si**3** oligomer may not be detected by UV absorption and ^{1}H NMR during the initial 20 min polymerization stage. These results are almost consistent with the time−conversion curves of the monomers. Therefore, we conclude that in the case of the Wurtz synthesis of PSi**1**, M**2** reacts with sodium before M**1** does.

Figure 7D shows the time−conversion curves of M**1** and M**3** from GC analysis for a reaction in the presence of 18-crown-6 (2.0 mol %) in toluene at 120 °C for 1 h. The curve clearly showes that ∼50% of M**3** reacted rapidly with sodium during the first 5 min and was completely consumed after 15 min, whereas ∼50% of M**1** reacted slowly over the first 10 min and

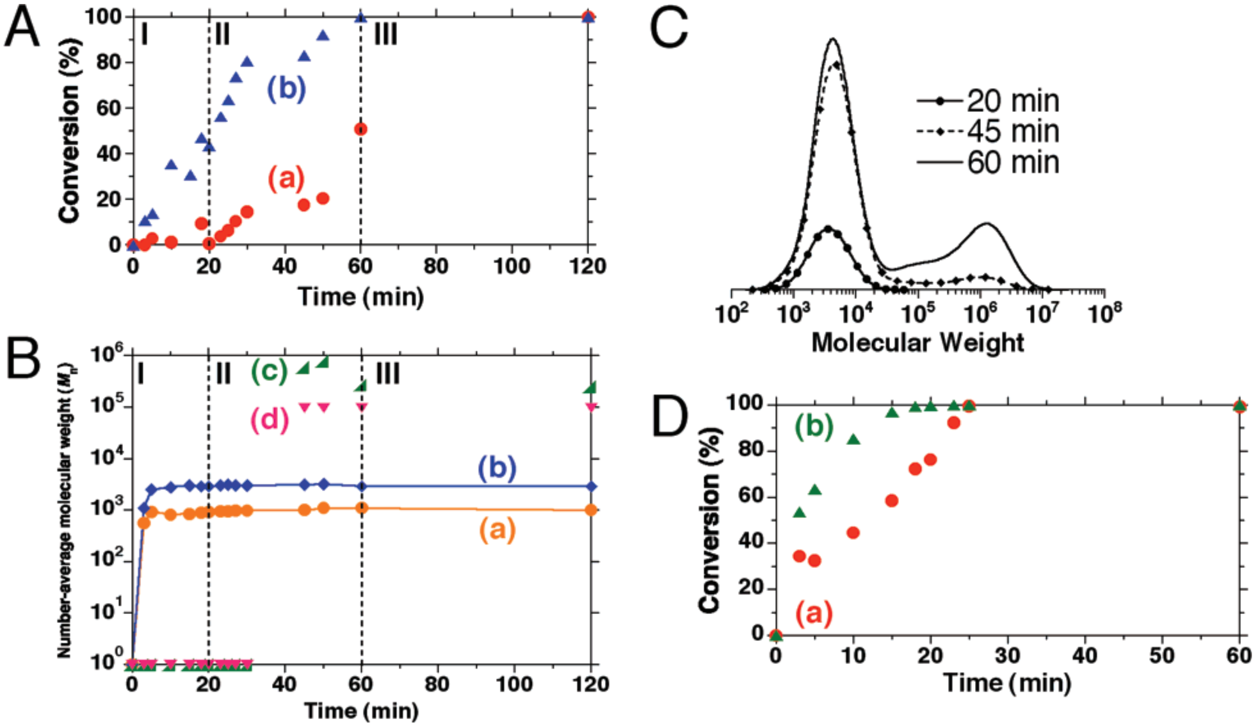

Figure 7. (A) Time−conversion curves for the Wurtz-type cocondensation reaction of (a) *i*-butyl-*n*-decyldichlorosilane (M**1**) and (b) methyl-3,3,3-trifluoropropyldichlorosilane (M**2**) without 18-crown-6 in toluene at 120 °C. Conversion was calculated based on crude total yields. (B) Variation with time of the products of (a) low-molecular weight species with UV absorption at 244 nm, (b) Si**4** oligomer with UV absorption at 292/295 nm, (c) PSi**1** with UV absorption at 303/307/311 nm, and (d) PSi**1** with UV absorption at 300 nm. (C) Molecular weight distributions for crude products of the Wurtz-type cocondensation reaction of M**1** and M**2** at 20, 45, and 60 min. (D) Time−conversion curves for the Wurtz-type cocondensation reaction of (a) *i*-butyl-*n*-decyldichlorosilane (M**1**) and (b) methyl-*n*-propyldichlorosilane (M**3**) with 18-crown-6 (2.0 mol % to comonomers) in toluene at 120 °C.

was completely consumed after 25 min. The ratio of the initial polymerization rate of M**3** to M**1** was ∼2. This suggests that M**1**, with its bulky *i*-butyl and long *n*-decyl groups, and M**3**, with its compact methyl and short *n*-propyl groups, showed a substantial difference in reactivity to sodium reduction to produce M**1**- and M**3**-based oligosilane blocks with polymerizable end group(s). In the particular case of PSi**1** synthesis, however, it seems likely that the electrostatic attractive force between sodium and the three F atoms of the trifluoropropyl group may be the dominant factor behind the substantial difference in the ease with which M**1** and M**2** are reduced by sodium.[29]

It is important to note that the viscosity of the reaction mixture greatly increased when PSi**3** was prepared by the Wurtz synthesis, due to the formation of high-molecular weight polymers ($10^5 \le M_w \le 10^6$). Indeed, the reaction solution eventually became a gel after prolonged polymerization. This was very similar to the case of PSi**1** synthesis. Although the marked increase in solution viscosity during PSi**1** synthesis was not recognized by the naked eye until ∼20 min into the reaction, the viscosity greatly increased between 20 and 60 min. It was during this same interval between ∼20 and 60 min that M**1** began to react with sodium. When ∼50% of M**1** was consumed after ∼60 min, the reaction solution reached the gel state. For simplicity and clarity, we classified the reaction processes into three stages: 0−20 min (stage I), 20−60 min (stage II), and 60−120 min (stage III) (Figure 7). Our proposed mechanism for the formation of multiblock PSi**1** (Figure 8) is based on product analysis during the three stages (I, II, III), along with previous studies of the Wurtz-type condensation reaction of dichlorosilanes.[30−32]

Stage I: The reactive M**2** (abbreviated as M_F in Figure 8) can initially react at the surface of sodium to form Si**4** oligomer (M_n= 3 000, *n*= 21). As the Wurtz-type condensation reaction proceeds, most Si**4** oligomers diffuse from the surface into bulk solution. These Si**4** oligomers can carry polymerizable terminal groups, such as silyl radicals, silyl anions, silyl anion radicals, and Si−Cl end groups. At the same time, cyclic oligosilanes may be produced by end-biting and back-biting reactions simultaneously, leading to no further polymerization.

Stage II: The less reactive M**1** (abbreviated as M in Figure 8) begins to react at the sodium surface when ∼50% of M**2** is consumed after ∼20 min. In this case, the large piece of sodium metal, which is several millimeters in diameter and visible with the naked eye, breaks into fine particles with a purple color, which react easily with M**1** without the help of cocatalysts.[33] If M**1** can react effectively with Si**4** oligomers with polymerizable functional groups at the sodium surface, the LMW products made from M**1** can be incorporated into PSi**1** as blocklike structures [Stage II, (a)]. In the same manner as for Si**4** oligomers, M**1** provides Si**3** oligomers carrying polymerizable functional groups. This Si**3** oligomer diffuses into the solution phase [Stage II, (b)]. If Si**3** oligomers in the solution phase can react with Si**4** oligomers not at the sodium surface but in the solution phase, blocklike structures can be produced without the help of sodium. One possibility for producing multiblock PSi in bulk solution may be to use chain carriers that are silyl radical and/or radicals located at the chain end(s) of these oligomers.

In a previous paper, we used NMR and IR spectroscopies to provide evidence of Si−H termini in several dialkylpolysilanes and we proposed that silyl radicals of propagating chain ends are responsible for Si−H termini via a hydrogen abstraction reaction.[34] West et al. reported that the dominant products in PSi synthesis are cyclic and chainlike oligosilanes.[1] Moreover, Jones et al. reported that the dominant products of the Wurtz

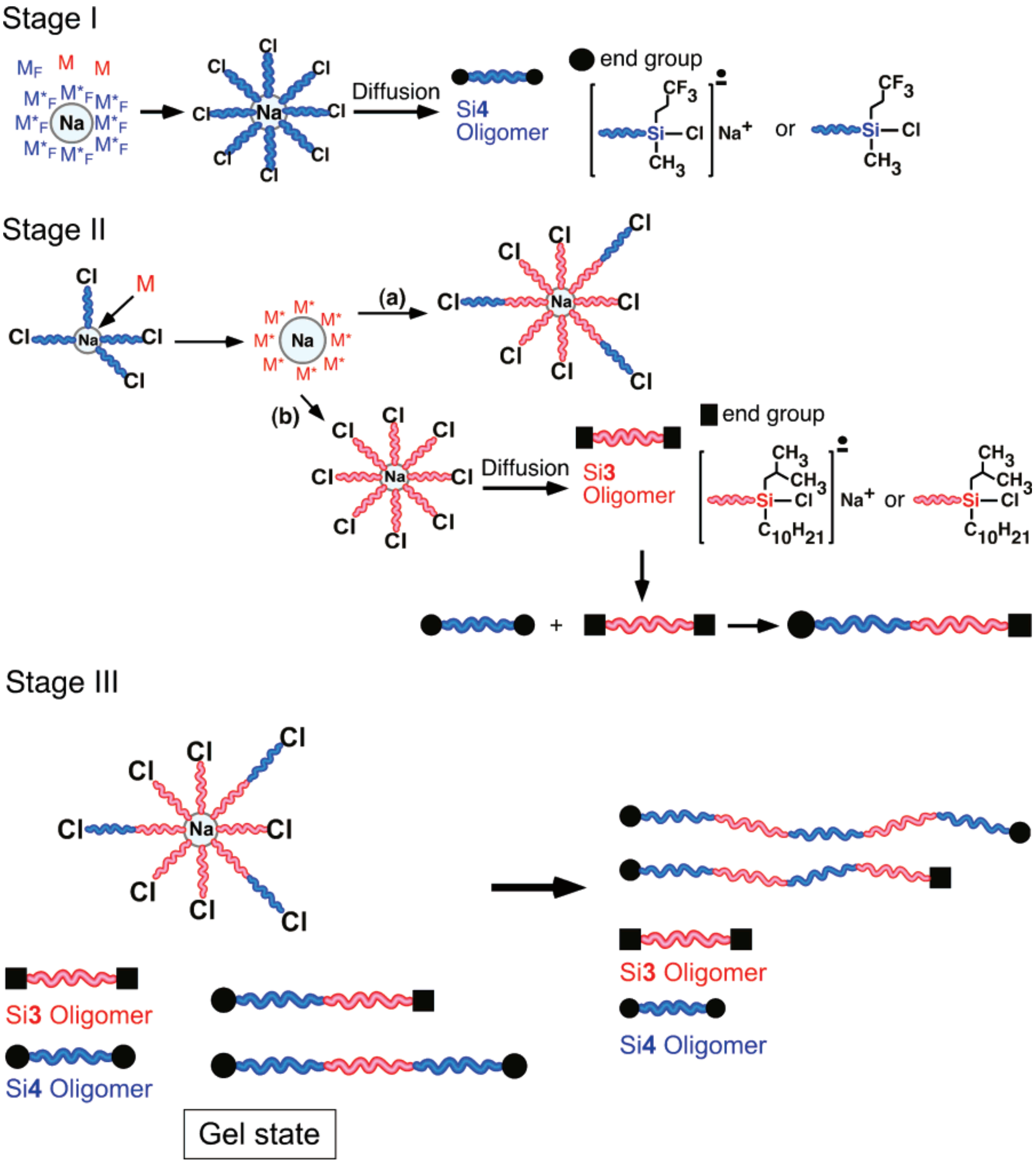

Figure 8. A proposed mechanism for the formation of the multiblock polysilane copolymer, poly[(*i*-butyl-*n*-decylsilane)$_x$-*b*-(methyl-3,3,3-trifluoropropylsilane)$_{1-x}$] (PSi**1**), by a Wurtz-type cocondensation reaction in toluene at 120 °C. Stage I, solution state; stage II, viscous solution state; and stage III, gel state. The mechanism was originally proposed by Jones et al.[30,32]

synthesis of poly(methylphenylsilane) (PMPS) are oligomeric polymers with $n = 35-40$.[30] Note that this value of n for PMPS is comparable to $n = 21$ for the Si**4** oligomer formed in stage I and $n = 19$ for the Si**4** blocks evaluated by the block-selective scission reaction. To effectively produce the blocklike PSi copolymers, it may be necessary to use two dichlorosilanes with markedly different reactivity toward reduction by sodium. This arrangement could thereby lead to effective production of two different types of oligosilanes bearing polymerizable end group(s).

Stage III: When the solution viscosity increases to the gel state, it is possible that oligomeric and polymeric species with polymerizable ends can react mutually and randomly to produce an HMW multiblock PSi**1** copolymer. The oligomeric and polymeric species include Si**3** oligomer, a medium molecular weight (MMW) Si**3** polymer, Si**4** oligomer, and a LMW multiblock PSi**1** copolymer.

Conclusion

The multiblock PSi copolymer, poly[(*i*-butyl-*n*-decylsilane)-*b*-(methyl-3,3,3-trifluoropropylsilane)] (PSi**1**), was produced in a one-pot Wurtz synthesis with *i*-butyl-*n*-decyldichlorosilane (**M1**) and methyl-3,3,3-trifluoropropyldichlorosilane (**M2**) comonomers with sodium in refluxing toluene. No cocatalysts or additives were used. The main chain structure of PSi**1** was characterized by ^{29}Si{^{1}H} NMR, UV absorption, PL, and PLE measurements. Using the block-selective scission technique with fluoride anion (F$^-$), average block lengths for the *i*-butyl-*n*-decylsilane (Si**3**) block and the methyl-3,3,3-trifluoropropylsilane (Si**4**) block were found to be ~4.8 nm (averaged repeating unit, $n = 26$) and ~3.5 nm ($n = 19$), respectively. The multiblock copolymerization behavior of PSi**1** was further elucidated by time–conversion curves of M**1** and M**2** in the polymerization reaction mixture by a GC technique. Product analysis of PSi**1** in the polymerization reaction mixture was carried out by ^{1}H NMR measurement and GPC equipped with a photodiode array UV detector. Upon simultaneous addition of M**1** and M**2**, M**2** immediately formed Si**4** oligomer (M_n = 3 000). After a polymerization time of 20 min, M**1** abruptly copolymerized with the Si**4** oligomer, and PSi**1** with a high molecular weight subsequently formed. On the basis of these results, we proposed a mechanism for the production of multiblock PSi copolymers via one-pot Wurtz synthesis. It appears that two dichlorosilanes with a marked difference in Wurtz reduction reactivity are needed to effectively produce two different types of oligosilanes carrying polymerizable end group(s) in bulk solution (not on the sodium surface). Furthermore, the blocklike nature of various dialkylsilane copolymers may be a feature common to one-pot Wurtz reduction of dialkyldichlorosilane comonomers.

Acknowledgment. The authors thank Prof. Tsuyoshi Kawai, Dr. Takuya Nakashima, and Takashi Terashima for guidance on computational calculations and many fruitful discussions. The authors also thank Prof. Masao Tanihara, Prof. Jun-ichi Kikuchi, Prof. Kotohiro Nomura, Dr. Hisanari Onouchi, and Masashi Nakamura for many fruitful discussions. M.N. and M.F. acknowledge support from the Grants-in-Aid for Scientific Research (Grant 16205017). M.N. and M.F. also acknowledge partial funding from the Scientific Research of Priority Areas program (Grant 446).

Supporting Information Available: Additional ^{29}Si{^{1}H} NMR spectra, PL and PLE spectra, ^{1}H and ^{19}F NMR spectra, plots of changes in molecular weight and UV absorbance, and HOMO and LUMO orbitals. This material is available free of charge via the Internet at http://pubs.acs.org.

References and Notes

(1) For a review, see West, R. *J. Organomet. Chem*. **1986**, *300*, 327−346 and references therein.
(2) For a review, see Miller, R. D.; Michl, J. *Chem. Rev.* **1989**, *89*, 1359−1410 and references therein.
(3) Naito, M.; Fujiki, M. *Soft Matter* **2008**, *4*, 211−223.
(4) West, R.; David, L. D.; Djurovich, P. I.; Stearley, K. L.; Srinivasan, K. S. V.; Yu, H. *J. Am. Chem. Soc.* **1981**, *103*, 7352−7354.
(5) West, R.; Wolff, A. R.; Peterson, D. J. *J. Radiat. Curing* **1986**, *13*, 35−40.
(6) Yajima, S.; Hayashi, J.; Omori, M. *Chem. Lett.* **1975**, 931−934.
(7) West, R.; David, L. D.; Djurovich, P. I.; Yu, H.; Sinclair, R. *Ceram. Bull.* **1983**, *62*, 899−903.
(8) Saxena, A.; Fujiki, M.; Rai, R.; Kim, S.-Y.; Kwak, G. *Macromol. Rapid Commun.* **2004**, *25*, 1771−1775.
(9) Saxena, A.; Rai, R.; Kim, S.-Y.; Fujiki, M.; Naito, M.; Okoshi, K.; Kwak, G. *J. Polym. Sci., Part A: Polym. Chem.* **2006**, *44*, 5060−5075.
(10) Wang, W-Z.; Fan, Q-L.; Cheng, F.; Zhao, P.; Huang, W. *J. Polym. Sci., Part A: Polym. Chem.* **2006**, *44*, 3513−3525.
(11) Gauthier, S.; Worsfold, D. J. In *Silicon-Based Polymer Science: A Comprehensive Resource*; Zeigler, J. M., Fearon, F. W. G., Eds.; Advances in Chemistry Series 224; American Chemical Society: Washington, DC, 1990; pp 299−307.
(12) Wesson, J. P.; Williams, T. C. *J. Polym. Sci., Polym. Chem. Ed.* **1981**, *19*, 65−72.
(13) Worsfold, D. J. In *Inorganic and Organometallic Polymers: Macromolecules Containing Silicon, Phosphorus, and Other Inorganic Elements*; Zeldin, M., Wynne, K. J., Allcock, H. R., Eds.; ACS Symposium Series 360; American Chemical Society: Washington, DC, 1988; pp 101−111.
(14) Wolff, A. R.; Nozue, I.; Maxka, J.; West, R. *J. Polym. Sci., Part A: Polym. Chem.* **1988**, *26*, 701−712.
(15) Sakamoto, K.; Yoshida, M.; Sakurai, H. *Macromolecules* **1990**, *23*, 4494−4496.
(16) Schilling, F. C.; Lovinger, A. J.; Davis, D. D.; Bovey, F. A.; Zeigler, J. M. *Macromolecules* **1992**, *25*, 2854−2859.
(17) Fujino, M.; Hisaki, T.; Matsumoto, N. *J. Polym. Sci., Part A: Polym. Chem.* **1995**, *33*, 2279−2283.
(18) Yamaguchi, S.; Akiyama, S.; Tamao, K. *J. Am. Chem. Soc.* **2000**, *122*, 6793−6794.
(19) Hiyama, T.; Obayashi, M.; Mori, I.; Nozaki, H. *J. Org. Chem.* **1983**, *48*, 912−914.
(20) Hiyama, T.; Obayashi, M.; Sawahata, M. *Tetrahedron Lett.* **1983**, *24*, 4113−4116.
(21) Fujiki, M. *J. Am. Chem. Soc.* **2000**, *122*, 3336−3343.
(22) Naito, M.; Saeki, N.; Fujiki, M.; Ohira, A. *Macromolecules* **2007**, *40*, 648−652.
(23) Fujino, M.; Hisaki, T.; Fujiki, M.; Matsumoto, N. *Macromolecules* **1992**, *25*, 1079−1083.
(24) Saxena, A.; Fujiki, M.; Naito, M.; Okoshi, K.; Kwak, G. *Macromolecules* **2004**, *37*, 5873−5879.
(25) Fujino, M.; Isaka, H. *J. Chem. Soc., Chem. Commun.* **1989**, 466−467.
(26) Gauthier, S.; Worsfold, D. J. *Macromolecules* **1989**, *22*, 2213−2218.
(27) Michl, J.; West, R. *Acc. Chem. Res.* **2000**, *33*, 821−823.
(28) Zhang, R. Q.; Zhao, Y. L.; Teo, B. K. *Phys. Rev. B* **2004**, *69*, 125319−125326.
(29) Plenio, H.; Hermann, J.; Diodone, R. *Inorg. Chem.* **1997**, *36*, 5722−5729.
(30) For a review, see Jones, R. G.; Holder, S. J. *Polym. Int.* **2006**, *55*, 711−718 and references therein.
(31) Jones, R. G.; Holder, S. J. In *Silicon-Containing Polymers: The Science and Technology of their Synthesis and Applications*; Jones, R. G., Ando, W., Chojnowski, J., Eds.; Kluwer Academic Publishers: Dordrecht, The Netherlands, 2000; pp 353−373.
(32) Jones, R. G.; Budnik, U.; Holder, S. J.; Wong, W. K. C. *Macromolecules* **1996**, *29*, 8036−8046.
(33) Benfield, R. E.; Cragg, R. H.; Jones, R. G.; Swain, A. C. *Nature* **1991**, *353*, 340−341.
(34) Saxena, A.; Okoshi, K.; Fujiki, M.; Naito, M.; Guo, G.; Hagihara, T.; Ishikawa, M. *Macromolecules* **2004**, *37*, 367−370.

MA702639F